10 be presented at the Fifth NASA Symposium on VLSI Design (Albuquerque, NM Nov. 4-5 '93).

STRV RADMON: AN INTEGRATED HIGH-ENERGY PARTICLE DETECTOR

Martin Buehler, George Soli, Brent Blaes, and Gemma Tardio

VLSI Technology Group
Jet Propulsion laboratory
California Institute of Technology
Pasadena, CA 91109

The RADMON (Radiation Monitor) was developed as a compact device with a 4-kbit SRAM particle detector and two p-FET total dose monitors, Thus it can be used as a spacecraft radiation alarm and in situ total close monitor. This paper discusses the design and calibration of the SRAM for proton, alpha, and heavy ion detection. Upset rates for the RADMON, based on a. newly developed space particle flux algorithm, are shown to vary over eight orders of magnitude. On the STRV (Space technology Research Vehicle) the RADMON's SRAM will be used to detect trapped protons, solar flares, and cosmic rays and to evaluate our ability to predict space results from ground tests.

1. MISSION OVERVIEW

The SIRV (Space-Technology Research Vehicle) consists of two spacecraft as shown in fig. 1. Each vehicle is approximately a cube 17 inches on a side that will be launched into a geosynchronous transfer orbit (GTO) with a 200-km perigee, a 36,000-km apogee, and an II-hour period, This orbit provides the opportunity to profile the Earth's radiation belts.

The SIRV contains a number of radiation measuring instruments including the JPL RADMON (Radiation Monitor), the DRA CREDO (Cosmic Environment Dosimeter), and the ESA REM (Radiation Environment Monitor), The CREDO and REM use PIN diodes or surface barrier (SB) detectors with pulse-height detection circuitry to discriminate particle energy. The area of the CREDO and REM detectors is between ?? to 400 mm^2; whereas, the area of the RADMON is only 0.17 mm^2. Thus the upset rates are much higher for the CREDO and REM than for the RADMON.

The purpose of this paper is to present the methodology for calculating the RADMON's upset rate using a newly developed algorithm for the space environment and the RADMON's device parameters. After launch, the upset rate for the CREDO, REM and RADMON will be compared to determine the validity of the ground predictions and the relative sensitivity of the three particle detectors.

The space particles relevant to RADMON upsets are: (a) trapped protons (TP), (b) galactic cosmic rays (GCRs), and (c) solar flare particles (SFP). Electrons in the electron belt will not upset the RADMON. Electrons provide a total dose which causes a slow drift in the RADMON baseline which is constantly monitored.

2. SEU SRAM

The RADMON, shown in Fig. 2, is a 28-pin chip with a 4-kbit SRAM for SEU (single-event upset) detection and two p-FETs [1] for total dose monitoring. The SRAM contains a six-transistor memory cell which is illustrated in the schematic cross section of Fig. 3. This figure shows that the memory cell has been modified in two ways to increase the cell's sensitivity to upsets. First, the drain area, a_m, of diode Dn2 has been increased to increase its particle capture cross section. Second, the diode Dn2 is biased with an offset voltage, V_o, which is applied through p-FET Mp2. This allows the cell to be operated near its metastable point which in turn allows the cell's upset sensitivity be adjusted via V_o.

The interaction of high-energy particles with the RADMON is described in terms of the various layers the particle passes through as seen in Fig. 4. In passing through the layers, the particle looses energy and in general increases its LET (linear energy transfer) or its ability to deposit charge. Thus knowing the thickness of the shield and device overlayer is key to calculating particle upset rates.

The response of the RADMON to protons is illustrated in Fig. 5 where 0.55, 1.0, and 2.0 MeV protons upset the cells. The figure also includes the spontaneous upset curve which has a mean value of $V_{os\mu}$. The spontaneous curve defines the metastable point for each of the SRAM cells. This curve represents the baseline for the device.

In operation the RADMON is operated at a V_o greater than $V_{s\mu}$ or $\delta V = V_{op\mu} - V_{os\mu}$ where $V_{op\mu}$ is the mean particle offset voltage defined by the $\sigma_m/2$ crossing point shown in Fig. 5. For the STRV, the RADMON is operated with three δV_o values corresponding to a proton threshold, an alpha particle threshold, and a heavy ion threshold. These thresholds are listed in Table 1.

The vertical axis of Fig. 5 displays the particle cross section. It is calculated using:

$$(1)\quad \sigma = N/(\phi_m \cdot t_m \cdot N_t)$$

where ϕ_m is the measured particle flux, t_m is the measurement time, and N_t is the number of bits in the SRAM in this case $N_t = 4096$. This equation is applicable for $N \ll N_t$ which is satisfied when the number of flipped bits is less than 10 percent of N_t. This equation indicates that the cross section is proportional to the number of flipped bits, N. The proportionality factor, the denominator, normalizes the data with respect to flux and measurement time.

In order to predict the RADMON's upset rate, σ_m, δQ_c, and $\delta X4$ must be known. The device cross section is taken from the physical layout and in this case $\sigma_m = 42.1$ μm^2. The critical charge is related to V_o through:

$$(2)\quad \delta Q_c = C_u \cdot \delta V_o$$

where C_u is the upset capacitance. The collection depth, $\delta X4$, is shown in Fig. 3. Both C_u and $\delta X4$ are determined experimentally and in this discussion C_u = 28.9 fC/V and $\delta X4$ = 2 μm are used.

The RADMON's proton response, shown in Fig. 5, reveals a non-monatonic behavior between the particle energy and δV_o. This behavior is explained by analyzing the proton charge depth curves [2] shown in Fig. 6. The vertical lines indicate the

width of the overlayer and the width of the collection depth; that is, δX_3 = 5.6 μm and δX_4 = 2 μm. The figure shows that the 0.55 MeV proton stops in δX_4 and the 1.0 and 2.0 MeV protons stop beyond δX_4. The 0.? MeV proton stops in the overlayer so it can not be detected. The explanation for the non-monatonic energy versus δV_0 behavior follows from the charge deposited in the collection layer, δQ_C, as indicated in Fig. 6. This charge is proportional to δV_0 as given in ['q. 2 and thus explains the non-monatonic behavior.

It is concluded that the SRAM detects protons in the 0.5 to 2.0 MeV range. Higher energy protons can be detected only if their energy is brought in to the detection range by using a shield which drops the proton energy into the 0.5 to 2.0 MeV energy range. The STRV contains 16 RADMONS; half are shielded by a 2.0-mm Al shield and the other half are shielded by a 5.5-mm Al shield. The effect of shielding on the detection of protons is discussed in a later section.

3. GALACTIC COSMIC RAY AND S01 AR f LARE PARTICl E UPSETS :

Galactic cosmic ray (GCR) and solar flare particle (SIP) upsets are illustrated in Fig. 7. These curves were obtained by fitting Adam's curves [3]; the GCR are for solar minimum conditions. The curves show that shielding has a significant effect on the SFPS but relatively little effect on the GCRs.

The number of upset per SRAM is given by:

$$(3)\quad u = N \cdot \Omega \cdot t \cdot \sigma_m \cdot F$$

where N is the number of bits per SRAM, Ω is the solid angle, t is the observation or stare time, σ_m is the area sensitive to upsets, and f is the integral particle flux. The Petersen Equation [4] is commonly used to calculate SRAM upsets. The flux expression is:

$$(4)\quad F(1/\mu m^2 \cdot ster \cdot sec) = 4.4 \times 10^{-12} / [L\ (MeV \cdot cm^2/mg)]^2$$

where 1 is the linear energy transfer. The conversion factor for L in silicon is $L(MeV \cdot cm^2/mg) = L(fC/\mu m)/10.25$ where $L(fC/\mu m) = \delta Q_C(fC)/\delta X_4(\mu m)$. The Petersen equation holds for a 0.63-mm Al shield in a 10 percent worse case environment (10%WC),

The effect of shielding on the particle flux was obtained by fitting the Adam's data [3]. The flux is:

$$(5)\quad F(1/\mu m\ 2 \cdot \$er.see) = F_0 \cdot (L/L_0)^{a+b \cdot LOG(1+D/Do)}$$

where D is the shielding thickness in g/en?. The shielding thickness is given by $(5X1 = D/\rho$ where ρ is the shield density in g/cm^2. The values for F_0, L., a, and b are listed in Table ?.

The upsets expected for the RADMON are shown in Fig. 8 where the three LET thresholds are labeled. For the SFPS the RADMON will experience numerous upsets during the 600 sec stare time, For the GCRS, the RADMON will experience less than one upset per 600 sec stare time, The results are summarized in Table 1.

4. PROTON BELT UPSETS:

The profile of the proton belt is shown in Fig. 9. It shows that the SIRV remains in the vicinity of proton belt peak for several hundred seconds. Before reaching the RADMON the protons must pass through the Al shields. From the proton range curves [2], it can be shown that the protons must have $E_0 > 18.5$ MeV to pass through a 2.0-mm Al shield and $E_0 > 32.5$ MeV to pass through a 5.5-mm Al shield. The proton energy must be lowered by the shield so that it has an energy between 0.5 and 2.0 MeV when it enters the RADMON'S collection in order to be detected. This effect is shown graphically in fig. 10 where two solid horizontal lines have been drawn at the bounds of the RADMON's detection range. The problem now is to determine δE_0, the incremental incident proton energy that can be detected by the RADMON.

The number of protons that upset the RADMON during the stare time, t, is:

$$(6) \quad N = \sigma_m \cdot \phi_d \cdot t \cdot N_t \cdot \delta E_0$$

where ϕ_d is the differential incident proton flux which is determined from the peak of the proton belt curves shown in Fig. 9. For $E_0 < 30$ MeV, $\phi_d = 600$ $p/(cm^2 \cdot sec \cdot MeV)$ and for $E_0 > 30$ MeV, $\phi_d = 200$ $p/(cm^2 \cdot sec \cdot MeV)$. The δE_0 is given by:

$$(7) \quad \delta E_0 = (dE_0/dE_1)\delta E_1$$

where δE_1 is the incremental exit proton energy. The dE_0/dE_1 is determined from the proton range curves shown in Fig. 10 where $dE_0/dE_1 = 0.36$ for both the 2.0- and 5.5-mm Al shields.

A value for δE_1 is obtained by assuming that most of the proton energy is lost in the shield and virtually none is lost in the chip overlayer. Thus $\delta E_{\sigma 1} = \delta E_2 = \delta E_3$ = 2.0 - 0.5 = 1.5 MeV. Using Eq. 7, $\delta E_0 = 0.54$ MeV for both Al shields. Thus the RADMON will detect protons through the 2.0-mm Al shield with $E_0 = 18.77 \pm 0.27$ MeV and and through the 5.5-rim Al shield with $E_0 = 32.77 \pm 0.27$ MeV. This shows that the RADMON is really and energy detector for high-energy protons.

The number of trapped-proton induced upsets, calculated using Eq. 6, is listed in Table 3. It shows that several hundred upsets can be expected near the peak of the proton belt. The above calculation does not include particle scattering in the Al shield. Including this effect will increase the number of upsets.

5. DISCUSSION:

The number of upsets estimated for the RADMON varies over eight orders of magnitude and depends on the type of the space environment encountered, The upset estimates depend on the accuracy of the environmental models and device parameters such as the collection depth. A simple algorithm was developed for estimating space particle flux that includes the effect of shielding. The flight of the RADMON on the STRV along with the CREDO and REM will provide data to quantify the sensitivity of the three particle detectors and validate ground predictions.

6. REFERENCES:

1. M. G. Buehler, B. R. Blaes, G. A. SoIi, and G. R. Tardio, "On-Chip p-MOSFET Dosimeter," submitted for publication IEEE Trans. on Nuclear Science (Dee 1993).

2. J. F. Ziegler, J. P. Biersack, and U. Littmark, The Stopping and Range of Ions in Solids, Pergammon Press (New York, New York, 1985).

3. J. H. Adams, "The Variability of Single Event Upsets Rates in the Natural Environment," IEEE Trans. on Nuclear Science, Vol. NS-30, 4473-3389 (1993).

4. [. 1. Petersen, J. B. Langworthy, and S. F. Diehl, "Suggested Single [vent Upset Figure of Merit," IEEE Trans. on Nut. Science, Vol . NS-30, 4533-4539 (1983).

7. ACKNOWLEDGMENTS : The research described in this paper was performed by the Center for Space Microelectronics Technology, Jet Propulsion laboratory, California Institute of Technology, and was sponsored by the Ballistic Missile and Defense Organization, Innovative Science and technology Office. The RADMONs were fabricated through MOSIS, 1S1, USC, The authors are indebted to E. J. Daly, ESA, for the data shown in Fig. 9 and for his observation that the RADMON detects high-energy protons that fall in a narrow band of energies. File: STRV3B04.DOC.

Table 1. RADMON Particle thresholds and LETs.

THRESHOLD	VDD v	Vosμ v	δV_o v	LET $MeV \cdot cm^2/mg$
PROTON	3	1.13'9	0.61	0.086"
ALPHA	3	1.139	0.?50	0.353
HEAVY	5	1.720	3.280	4.6?8

Table ?. GCR and LSF Flux Parameters

PARAMETER	UNITs	GCR	LSF
F_o	$1/(\mu m^2 \cdot ster \cdot sec)$	$1x10^{-5}$	$1X10^{-2}$
L_o	$MeV \cdot cm^2/mg$	$1x10^{-4}$	$1x10^{-3}$
Do	mg/cm^2	78.36	0.5990
a	unitless	-1.92	-1.425
b	unitless	-1.35	-0.974

Table 3. RADMON Anticipated Upset Rates

ENVIRONMENT	PROTON BELT U(upsets/SRAM)	SOLAR FLARE U(upsets/SRAM)	10% WORSE CASE U(upsets/SRAM)	GCR U(upsets/SRAM)
Al-SHIELD	2.0-mm 5.5-mm	2.0-mm 5.5-mm	0.63-mm	2.0-mm 5.5-rim
PROTON	3.3E+2 1.1E+2	1.7E+3 5.4E+2	1.93E-1	7.5E-3 7.2E-3
ALPHA		1.5E+2 3.5E+1	1.15E-2	5.0E-4 4.7[-4
HEAVY		2.0E+0 2.3E-1	6.68E-5	3.6E-6 3.3E-6

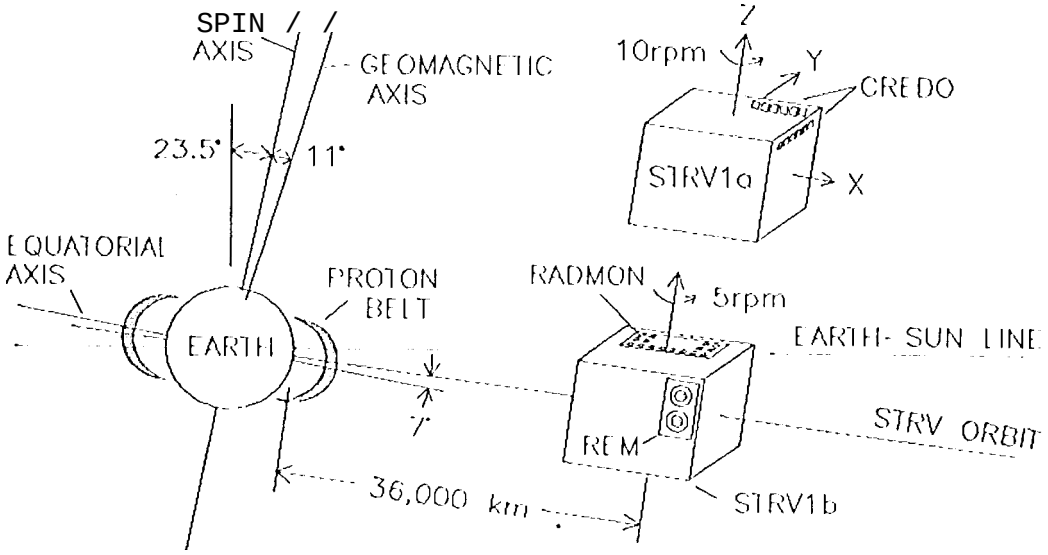

EARTH RADIUS = 6.371 km
PERIGEE = 200 km
APOGEE = 36,000 km
STRV2A27.FL1

Figure 1. STRV orbit relative to the earth's proton belt.

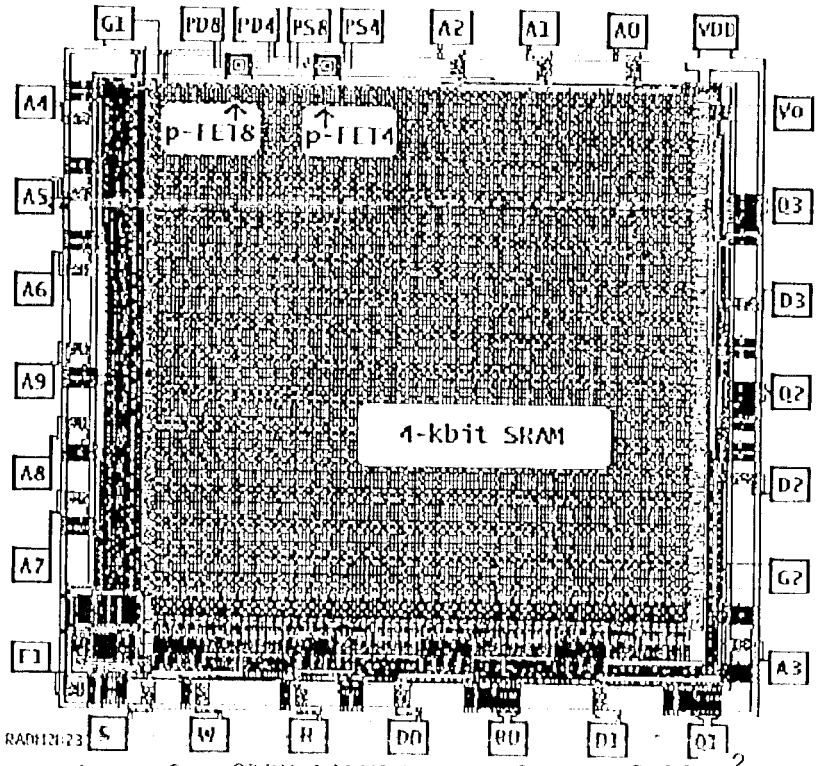

Figure 2. STRV-RADMON chip 2.57 x 2.70mm^2.

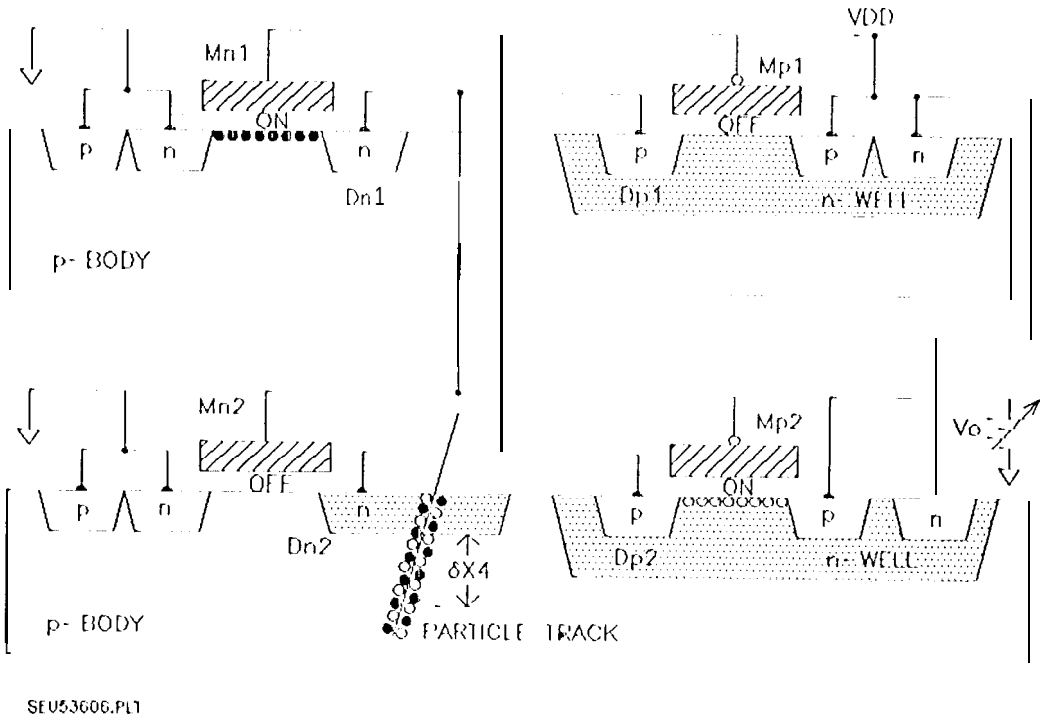

Figure 3. Cross section of SEU-SRAM showing a particle track through diode Dn2 which can cause a bit flip if sufficient charge is deposited.

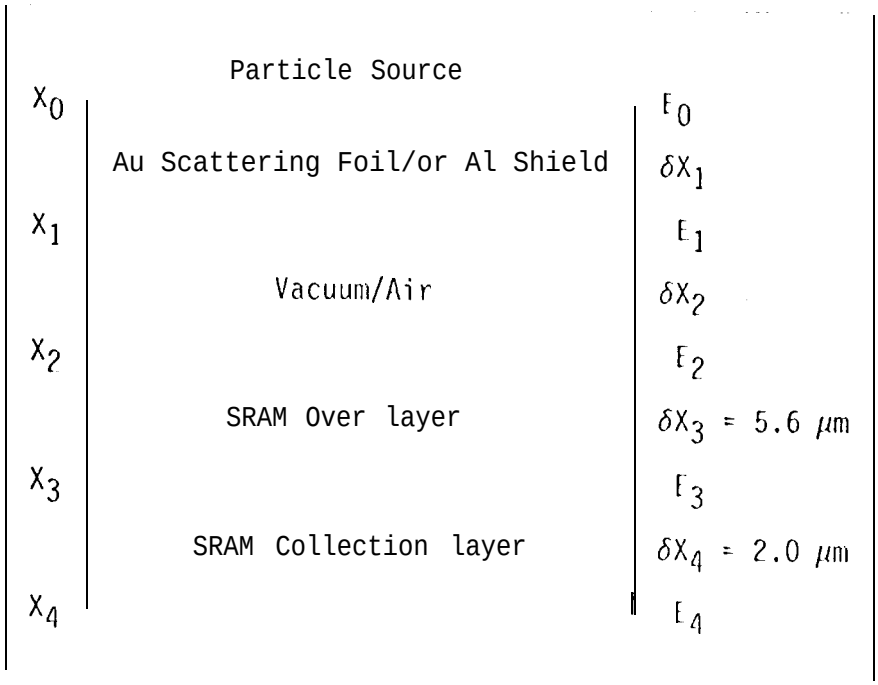

Figure 4. Schematic view of the particle path from the source to the SRAM.

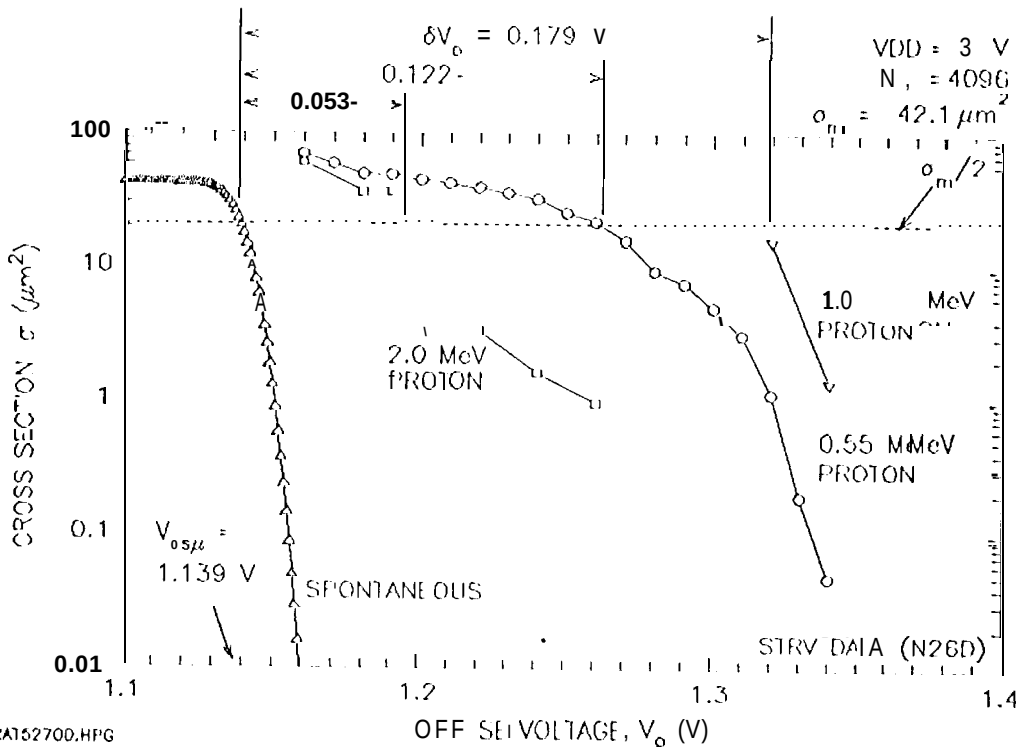

Figure 5. SRAM cross section/bit for protons with three different incident energies ($E_1 = E_2$).

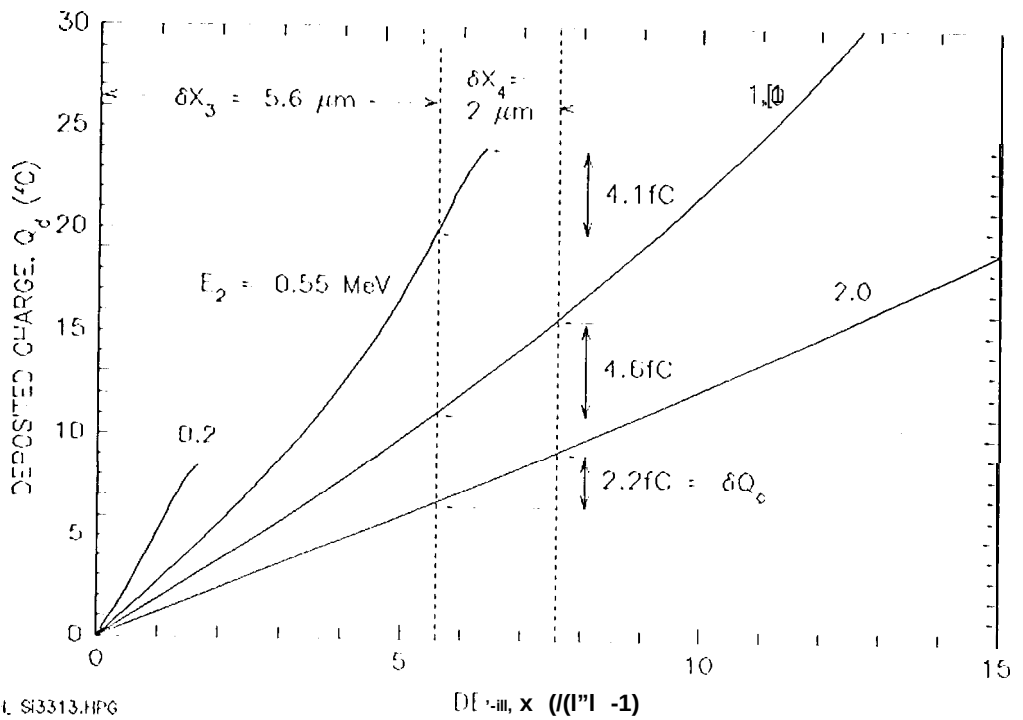

Figure 6, Proton charge deposited in si 1 icon [?] .

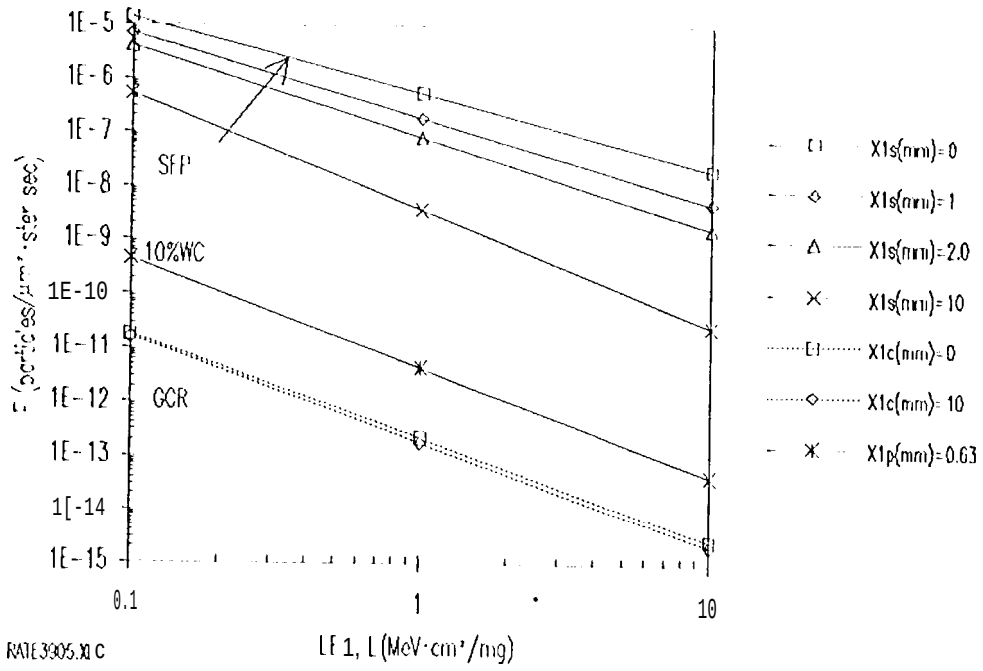

Figure 7, Integral LET interplanetary spectra for various aluminum shields [3] due to galactic cosmic rays (GCR), 10 percent worse case environment (10%WC), and solar flare particles (SFP).

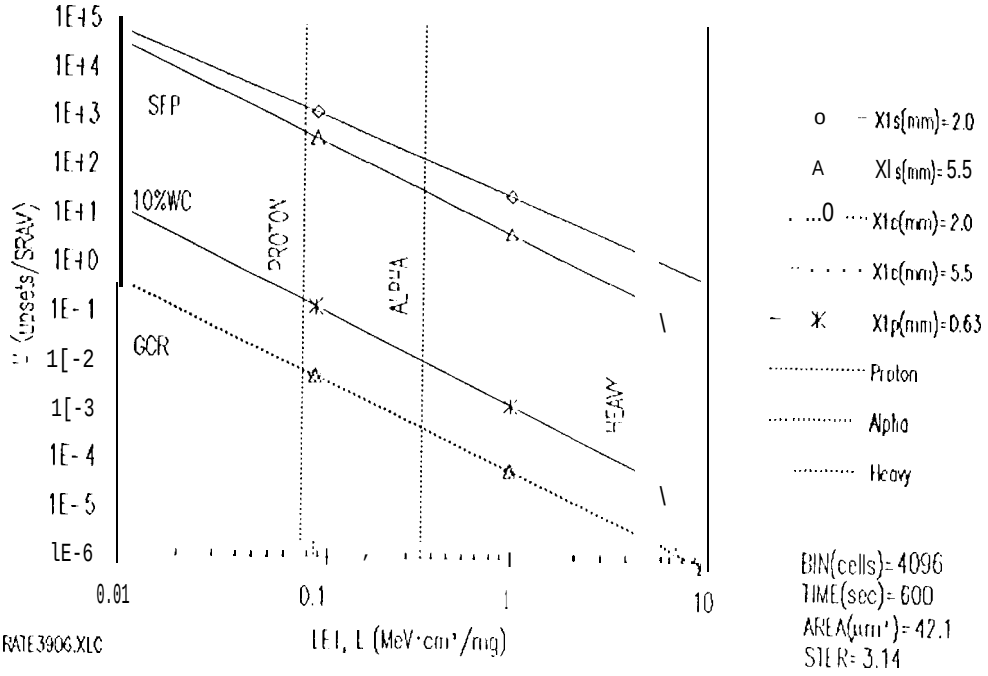

Figure 8. SIRV RADMON SEU SRAM upset rate due to galactic cosmic rays (GCR), 10 percent worse case environment (10%WC), and solar flare particles (SIP).

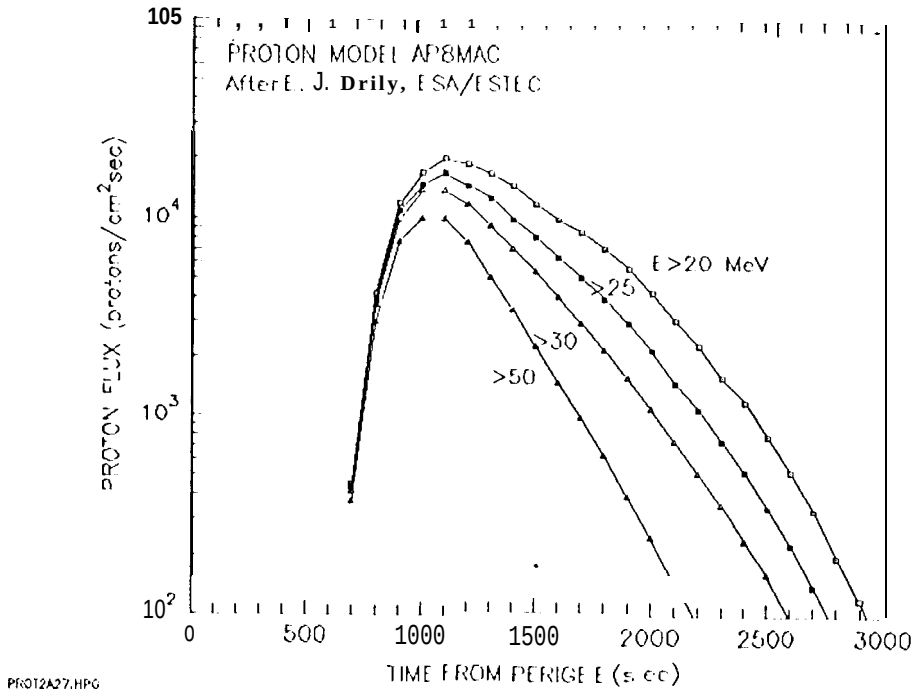

Figure 9. STRV traverse of the earth's proton belt.

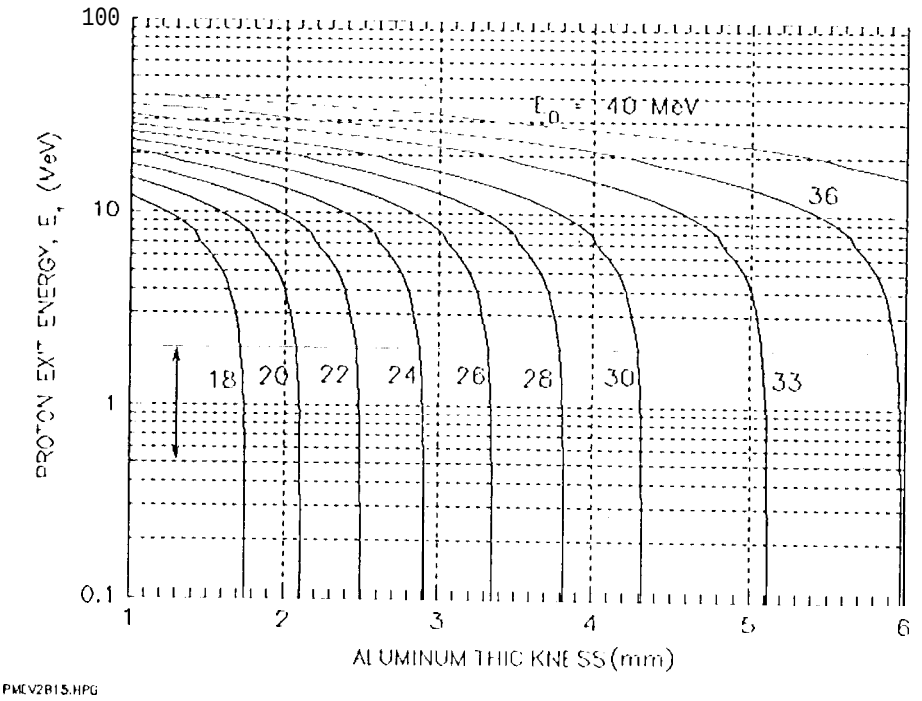

Figure 10. Proton exit energies for various aluminum thickness and incident proton energies, For X_{Al} = ? mm, E_0 ≈ 20 MeV and for X_{Al} = 5.5 mm, E_0 ≈ 35 MeV.